

## Relative Refractory Period in an Excitable Semiconductor Laser

F. Selmi, R. Braive,<sup>\*</sup> G. Beaudoin, I. Sagnes, R. Kuszelewicz, and S. Barbay<sup>†</sup>

*Laboratoire de Photonique et de Nanostructures, LPN-CNRS UPR20, Route de Nozay, 91460 Marcoussis, France*

(Received 19 December 2013; published 7 May 2014)

We report on experimental evidence of neuronlike excitable behavior in a micropillar laser with saturable absorber. We show that under a single pulsed perturbation the system exhibits subnanosecond response pulses and analyze the role of the laser bias pumping. Under a double pulsed excitation we study the absolute and relative refractory periods, similarly to what can be found in neural excitability, and interpret the results in terms of a dynamical inhibition mediated by the carrier dynamics. These measurements shed light on the analogy between optical and biological neurons and pave the way to fast spike-time coding based optical systems with a speed several orders of magnitude faster than their biological or electronic counterparts.

DOI: [10.1103/PhysRevLett.112.183902](https://doi.org/10.1103/PhysRevLett.112.183902)

PACS numbers: 42.65.Sf, 42.55.Px, 42.55.Sa, 87.19.II

Excitable response is a striking and generic response encountered in vastly different nonlinear systems from biology [1] to chemistry [2] and optics [3]. It can be phenomenologically described as an all-or-none type of response to an input perturbation: below the excitable threshold, the system responds linearly with a very small amplitude; above the excitable threshold, it gives birth to a large amplitude, nonlinear response whose shape and amplitude are almost independent from the input perturbation. In neurons, it is well known that the action potential that propagates along the axons has an excitable character [4]. Since excitability is at the base of the enormous processing capabilities of the brain, it has become a subject of study in nanoelectronics [5] as well as in photonics and nanophotonics with the goal to build neural networks architectures for computing [6].

As a standard test for excitability it is usually shown that the amplitude of the response versus the perturbation amplitude exhibits a steplike behavior. However, there exists another important property of excitable systems which is the existence of a refractory period. The refractory period is the time period following a first firing pulse during which the system cannot be excited anymore and is the crucial property responsible for the symmetry breaking phenomenon allowing the unidirectional propagation of activity pulses. This was already noted in [7] where a model for a population of spiking neurons with a refractory period but without firing threshold evidences stable propagation of activity pulses. From a signal processing point of view, should it regard excitable logic, cognitive processing, or pulse reshaping, the ultimate processing speed of optical or electronic systems depends also crucially on this parameter. In neuron physiology or dynamics textbooks, one usually makes the distinction between the absolute and the relative refractory periods. During the absolute refractory period, the inhibition is complete, while in the relative refractory period, an activity pulse can be emitted for a sufficiently high perturbation

amplitude. These periods correspond, respectively, to the depolarization of the axon membrane during the activity pulse buildup, and to the repolarization and hyperpolarization recovery at the end and after the activity pulse has reached its maximum amplitude. During the relative refractory period the amplitude of the second response pulse is lower than that of the first one because of inhibition effects.

In optics, excitable responses have been demonstrated in many different systems and configurations, and in particular in semiconductor-based systems where one can benefit from fast response time scales and small footprint [8–17]. However, if the absolute refractory period has been sometimes measured or studied, it has not yet been the case for the relative refractory period and the associated inhibitory effects.

In this Letter, we study the absolute and relative refractory periods in a micropillar laser with a saturable absorber. We demonstrate the existence of a very fast excitable response pulse ( $\sim 250$  ps), together with the characterization of the absolute and relative refractory periods. In analogy with the dynamics observed in real neurons, we demonstrate the inhibitory role of the carrier population dynamics and gain physical insight on the origin of both refractory periods by comparing the experimental results to a standard model of a laser with saturable absorber.

Semiconductor lasers with saturable absorber can build fast excitable units and allow subnanosecond excitable pulses as measured in planar systems [15]. Moreover, the micropillar laser design [18] allows for a compact system amenable to integration or to coupling of a large number of excitable unit cells with even shorter response times because of the smallness of the cavity and of the shortened material recombination times. Our excitable system is an optically pumped, micropillar laser embedding in its cavity center an active and a passive zone, thanks to an original design [19]. The active and the passive zones consist of, respectively, two and one InGaAs/AlGaAs quantum wells placed at the

antinode of the field at cavity resonance (980 nm). By a careful engineering of the multilayer stack, an external optical pump emitting around 800 nm can be absorbed in the active zone and not in the passive zone, thus playing the role of a saturable absorber. The 4  $\mu\text{m}$  diameter micropillar laser is fabricated by etching with inductively coupled plasma. The bottom mirror is only partially etched to prevent the pump laser, possibly wider than the micropillar diameter, from reaching the absorbing substrate and generating heat. A thick layer of SiN is then evaporated on the micropillar to protect the stack from oxidation and increase lateral heat dissipation. The index contrast between the semiconductor and the SiN layer remains sufficiently high for the field confinement to be unaffected by the presence of this layer. A second plasma-assisted (anisotropic) etching of the dielectric layer is conducted until the top of the micropillar is completely uncovered, leaving approximately a 2  $\mu\text{m}$  thick SiN layer around the micropillar (Fig. 1). The micropillar is optically pumped with a diode-array laser emitting at 794 nm. Optical perturbations are produced by a 80 MHz model-locked Ti:Sa laser emitting in the pump window around 800 nm. Its repetition rate is controlled by a pulse picker and the measured pulse duration is 80 ps.

We first study the excitable response of the micropillar under a single pulse excitation. In excitable lasers with SA, the self-pulsing regime occurs immediately at laser threshold through a homoclinic bifurcation [20] and the system is excitable for a bias pump below the laser threshold. Perturbation pulses of varying amplitudes are thus sent onto the micropillar optically biased in the excitable regime. The response amplitudes are detected with a 5 GHz bandwidth avalanche photodetector and acquired on a 6 GHz bandwidth oscilloscope. We acquire about  $10^4$  perturbation pulses and measure the maximum of the responses. The median of the results is calculated and displayed on Fig. 2(a). The median is chosen here instead of the mean because it is a more robust statistical indicator, in particular

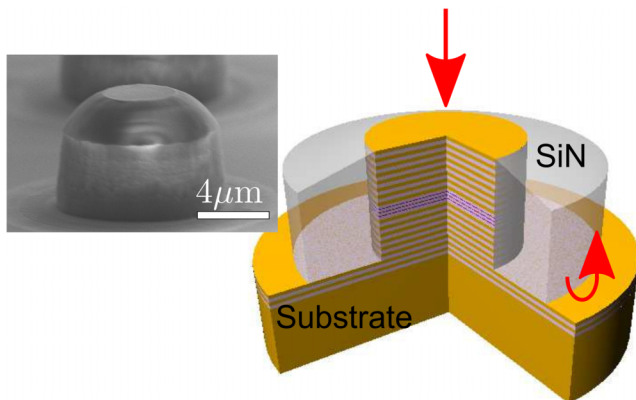


FIG. 1 (color online). Sketch and scanning electron microscope (SEM) image of the micropillar laser with saturable absorber (see text). Pump light (red arrow) is incoming from the top and is partially reflected from the remaining part of the lower Bragg mirror.

since we know the system's response is very sensitive to noise at the excitable threshold as was already studied in [15]. The response exhibits a typical excitable behavior with a sharp jump. It is well understood [15,21] and corresponds to the crossing of the unstable manifold emanating from the saddle point created when the system is close to a homoclinic bifurcation. As the bias pump intensity decreases, the excitable threshold increases and the amplitude of the response decreases as well, until there is no more jump at threshold, which corresponds to the disappearance of the excitable behavior. This demonstrates clearly the static control of the excitable threshold with the bias pumping. The dependence of the excitable threshold value with the pump level is linear as shown in inset of Fig. 2(a), for bias pumps not too far from the laser threshold. For lower pump values it becomes difficult to identify the excitable threshold because the fluctuations in the response become of the same order as the response jump. However, at very low pump powers ( $P = 0.2P_{SP}$ ), the excitable character completely disappears and the system enters the standard laser regime, thus displaying gain switching.

We split the input perturbation in two and introduce a variable delay in one of the optical paths to generate two consecutive pulses. Both perturbation pulse amplitudes are set to twice the excitable threshold to a single input perturbation pulse so that, when acting alone, each pulse gives the same response amplitude. We then monitor the amplitude of both pulses (Fig. 3) for time delays between 194 and 508 ps. One notes a decrease in the response amplitude to the second perturbation for short delays. When the second perturbation pulse becomes close enough to the first one, the amplitude of the response to the second

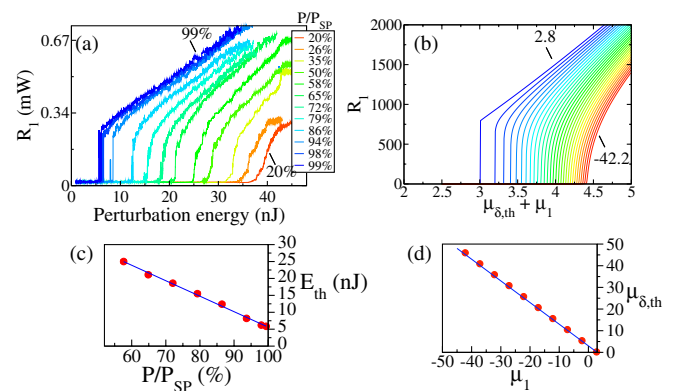


FIG. 2 (color online). (a) Amplitude of the response  $R_1$  to a single pulse perturbation versus perturbation energy  $E$  for varying bias pump  $P$  relative to the self-pulsing threshold  $P_{SP} = 694$  mW. (b) Theoretical response amplitude  $R_1$  to single input  $\delta$ -perturbation pulse  $\mu_\delta$  for different bias pumps  $\mu_1$  ranging from 2.8 to  $-42.2$ . Note that the curves are offset by  $\mu_1$  for clarity. (c) Dependence of the excitable threshold  $E_{th}$  (red circles) with reduced bias pump  $P/P_{SP}$  and linear fit (blue line). (d) Excitable threshold  $\mu_\delta$  versus bias pump  $\mu_1$ . The blue line is the theoretical approximation given by  $-\mu_1 + 1 + \mu_2$ .

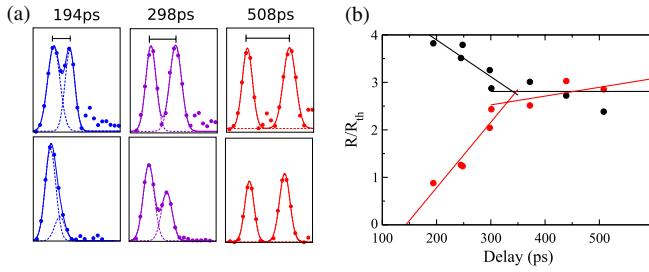


FIG. 3 (color online). (a) Recorded time traces for different delays and their Gaussian fits. Upper traces are the input perturbations and the lower traces are the system's response. The bias pump is set to 71% of the SP threshold. (b) Amplitude of the response  $R$  to the first (black) and second (red or gray) perturbation pulses for a double-pulse perturbation with variable delays.  $R_{th}$  is the response amplitude at the excitable threshold. Lines are linear fits in selected ranges and are guides for the eye.

perturbation pulse decreases abruptly, while the first pulse amplitude increases because of the interaction with the rising front of the second perturbation pulse. For a delay of the order of 150 ps we anticipate a total disappearance of the response, that marks the onset of the absolute refractory period (close to the excitable pulse duration of 190 ps). For delays between 150 and 350 ps, the response of the second pulse is inhibited and its amplitude is lower than for longer delays. The system is therefore in the relative refractory period. To check for the excitable character in this regime, we have performed measurements with a fixed perturbation amplitude of the first pulse and a varying perturbation amplitude of the second pulse. Indeed, it is known that a standard, nonexcitable, laser can show inhibition of the second response pulse when excited by two consecutive pulses. The results are shown on Fig. 4(a). If the second perturbation pulse arrives after a sufficiently long time, the system keeps an excitable character with a steplike response. As the delay decreases, the excitable threshold has a tendency to increase and the amplitude of the excitable response decreases. For a 530 ps delay, however, the response of the system is clearly not excitable anymore.

To gain more insight into the observed dynamics, we will compare our results to a standard rate equations model of a laser with SA. We introduce the Yamada model with spontaneous emission as in [20]. This model has already proved very accurate in describing the dynamics of semiconductor lasers with SA. It has also been recently recognized [22] as being an optical analog to the leaky integrate-and-fire neuron model in the limit of an infinitely fast photon cavity lifetime, a model widely used in computational neuroscience [23]. The model writes

$$\begin{aligned}\dot{I} &= I(G - Q - 1) + \beta_{sp}(G + \eta_1)^2, \\ \dot{G} &= b_1[\mu_1 - G(1 + I)], \\ \dot{Q} &= b_2[\mu_2 - Q(1 + sI)].\end{aligned}\quad (1)$$

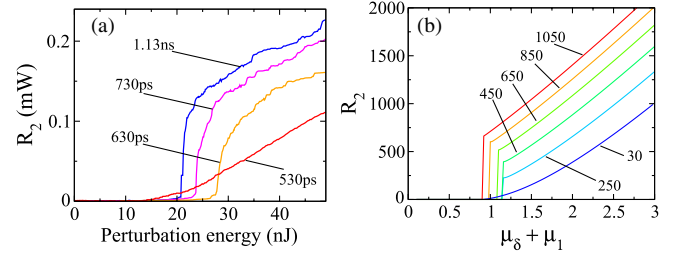


FIG. 4 (color online). (a) Experimental measurements of the amplitude of the response to a second perturbation pulse after a first pulse has been sent at  $t = 0$  whose amplitude is 20% above the excitable threshold and has triggered an excitable response, for different delays between the two pulses. Bias pumping is  $0.71P_{SP}$ . (b) Same as (a) according to the model [Eqs. (1)]. Time is rescaled to photon lifetime.

It consists of three coupled nonlinear ordinary differential equations for the intracavity intensity  $I$ , and the scaled excess carrier densities with respect to transparency in the gain and in the SA region  $G$  and  $Q$ . Other parameters are  $\mu_1$  the pumping intensity,  $\mu_2$  the nonsaturable losses,  $s$  the saturation parameter,  $\beta_{sp}$  the spontaneous emission factor, and  $\eta_1$  the transparency offset of gain. Time is rescaled to the cavity lifetime ( $\sim 1.3$  ps here) and  $b_{1,2}$  are the rescaled recombination rates of carriers in the gain and SA region. We take  $b_1 = 0.001$ ,  $b_2 = 0.002$ ,  $\mu_2 = 2$ ,  $s = 10$ ,  $\eta_1 = 1.6$ , and  $\beta_{sp} = 10^{-5}$ . These parameters are calculated from standard semiconductor laser parameters [15] and the recombination time scales are adjusted to match the observations. In the absence of spontaneous emission ( $\beta_{sp} = 0$ ), the system admits  $\{I = 0\}$  as invariant manifold. Therefore, any perturbation on the slow variables  $G$  or  $Q$  has no effect and the only way to trigger an excitable pulse is by perturbing the laser intensity itself by injecting resonant light into the cavity mode. In order to account for the experimental observations we include a spontaneous emission term. Hence, the steady state intensity below threshold is not zero anymore and the system is sensitive to perturbations on the pump. The steady state of the system ( $I_{ss}$ ,  $G_{ss}$ ,  $Q_{ss}$ ) can be simply evaluated by using a perturbation expansion in the small parameter  $\beta_{sp}$ :  $I_{ss} = \sum_{i=0}^{\infty} I_{ss,i} \beta_{sp}^i$  and identically for  $G_{ss}$  and  $Q_{ss}$ . We obtain at order 1 in  $\beta_{sp}$ :  $I_{ss} = \beta_{sp} I_{ss1}$ ,  $Q_{ss} = \mu_2(1 - \beta_{sp}s I_{ss1})$  and  $G_{ss1} = \mu_1(1 - \beta_{sp} I_{ss1})$  with  $I_{ss1} = (\mu_1 + \eta_1)^2 / (1 + \mu_2 - \mu_1)$ . Using the results derived in [20], we can find an approximation to the excitable threshold  $\mu_{\delta,th}$  for a delta perturbation at  $t = 0$  on the pump of amplitude  $\mu_{\delta}$  such that  $\mu_1 \rightarrow \mu_1 + \mu_{\delta} \delta(t)$  and we get  $\mu_{\delta,th} \approx -\mu_1 + 1 + \mu_2$ . The excitable threshold decreases linearly with increasing bias pump  $\mu_1$  and is independent of  $s$  at lowest order. This is due to the fact that during the initial phase after the perturbation the intensity is very small and hence doesn't have a great impact on the threshold. The results of the numerical simulation of the single pulse response amplitude versus

pump perturbation amplitude are shown on Fig. 2(b). The model shows the overall behavior already discussed and is in good qualitative agreement with the experimental results on Fig. 2(a).

The same model was used to characterize double pulse excitation response and the result is shown in Fig. 4(b). The qualitative agreement between the model with the experimental results on Fig. 4(a) is very good, though the predicted time scales are notably shorter and would certainly require a more elaborate model and more accurate semiconductor parameters. When the second perturbation pulse arrives long after the first excitable pulse has fired, the response is not affected and a second excitable pulse is emitted. When it arrives earlier in a delay such that the carriers did not have enough time to relax to their steady state values, the response level decreases (relative refractory period) until being completely repressed for a sufficiently small delay time (absolute refractory period). Note also the disappearance of the discontinuous response to the second perturbation, marking the fact that the system is not excitable anymore in this domain.

Our model reveals the underlying physical mechanism driving the system response. It shows that the response can be understood simply in terms of gain and carrier dynamics. Indeed, the second pulse acts as a probe for the gain and carrier dynamical evolution and the system reacts in a manner similar to the static case: whether a second excitable pulse emission occurs depends on the gain and SA depletion level at the arrival of the second perturbation. This is illustrated in Fig. 5.

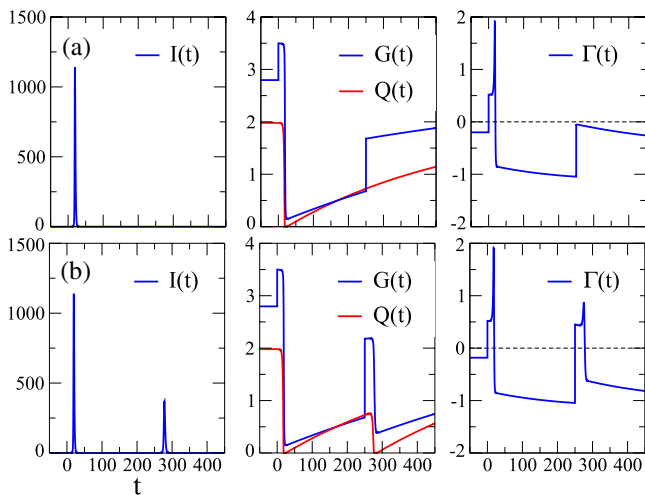


FIG. 5 (color online). Intensity  $I(t)$ , recovery dynamics of carriers  $G(t)$ ,  $Q(t)$  and net gain  $\Gamma(t)$  for a double delta perturbation at  $t_0 = 0$  and  $t_1 = 250$ . The first perturbation has amplitude  $\mu_\delta(t_0) = 3.5$  while the second perturbation is below (a),  $\mu_\delta(t_1) = 1.0$ , and above (b),  $\mu_\delta(t_1) = 1.5$ , the excitable threshold. Other parameters are unchanged. The initial state is the steady state.

After the first pulse is emitted the recovery of both carrier densities takes place. In the absence of any pulse the intensity is very small and can be neglected during part of the recovery dynamics, after the first pulse has fired. Hence, the evolution of the net gain  $\Gamma(t) = G(t) - Q(t) - 1$  is simply given by a combination of exponentials. When the second perturbation arrives, a pulse is emitted only if the intensity experiences a positive net gain for a sufficiently long period of time, i.e., if  $\Gamma(t)$  reaches positive values. Obviously since the carrier densities have not reached steady state and are depleted, the second pulse intensity is lower than the first: this is the relative refractory time. If the second pulse arrives after the carrier recovery is complete, a pulse with identical intensity can be triggered and one can consider that the system has left the refractory period regime.

It is fundamental to note that the relative refractory period and the inhibition of the response hold for any kind of perturbation, and in particular for a perturbation at the wavelength of the laser field. The advantage of using a perturbation on the pump is the relative insensitivity of the perturbation wavelength to the cavity resonance wavelength, which shifts with the pump bias intensity and may also shift dynamically with the carrier dynamics. This shift may be due to either thermal or carrier effects, and would make the experiments extremely difficult to perform and analyze. Moreover, this scheme allows us to clearly decouple the excitation and the response by filtering the output intensity.

In conclusion, we have analyzed the response of an excitable semiconductor system to single and double pulse excitations. In the single pulse excitation regime we have evidenced response times of the order of 200 ps and we have shown the inhibitory role of the pump. In the double excitation regime, we have evidenced the absolute and relative refractory periods, for delays below 200 ps and in the 200–350 ps range, respectively, and shown how they can be understood in terms of a dynamic inhibition mediated by the carrier dynamics recovery. We believe that these results pave the way to fast spike-time coding applications for optical cognitive computing [22], either by setting new constraints on the spike rate or enabling new functionalities. They also unveil the very similar behavior of the semiconductor laser with saturable absorber and the spiking neurons, making the former an ideal platform to study the neuromimetic dynamics of an ensemble of connected unit excitable cells or the propagation of excitable optical nonlinear waves [24]. This can be realized using coupled micropillar cavities [25,26] that can be arranged in various topologies.

We thank J. Bloch and A. Yacomotti for critical reading of the manuscript and for valuable comments and suggestions. This work was partially supported by the French Renatech network and by the ANR Blanc project Optiroc.

- \*Also at Université Paris Diderot, 5 rue Thomas-Mann, 75013 Paris, France.  
†sylvain.barbay@lpn.cnrs.fr
- [1] J. D. Murray, *Mathematical Biology* (Springer, New York, 1990).
- [2] A. Pacault, P. Hanusse, P. De Kepper, C. Vidal, and J. Boissonade, *Acc. Chem. Res.* **9**, 438 (1976).
- [3] F. Plaza, M. G. Velarde, F. T. Arecchi, S. Boccaletti, M. Ciofini, and R. Meucci, *Europhys. Lett.* **38**, 85 (1997).
- [4] E. Izhikevich, *Dynamical Systems in Neuroscience: The Geometry of Excitability and Bursting*. (The MIT press, Cambridge, MA, 2007).
- [5] S. H. Jo, T. Chang, I. Ebong, B. B. Bhadviya, P. Mazumder, and W. Lu, *Nano Lett.* **10**, 1297 (2010).
- [6] W. Maass, T. Natschläger, and H. Markram, *Neural Comput.* **14**, 2531 (2002).
- [7] W. M. Kistler and W. Gerstner, *Neural Comput.* **14**, 987 (2002).
- [8] M. Giudici, C. Green, G. Giacomelli, U. Nespolo, and J. R. Tredicce, *Phys. Rev. E* **55**, 6414 (1997).
- [9] H. J. Wünsche, O. Brox, M. Radziunas, and F. Henneberger, *Phys. Rev. Lett.* **88**, 023901 (2001).
- [10] S. Barland, O. Piro, M. Giudici, J. R. Tredicce, and S. Balle, *Phys. Rev. E* **68**, 036209 (2003).
- [11] F. Marino and S. Balle, *Phys. Rev. Lett.* **94**, 094101 (2005).
- [12] D. Goulding, S. P. Hegarty, O. Rasskazov, S. Melnik, M. Hartnett, G. Greene, J. G. McInerney, D. Rachinskii, and G. Huyet, *Phys. Rev. Lett.* **98**, 153903 (2007).
- [13] S. Beri, L. Mashall, L. Gelens, G. V. der Sande, G. Mezosi, M. Sorel, J. Danckaert, and G. Verschaffelt, *Phys. Lett. A* **374**, 739 (2010).
- [14] A. M. Yacomotti, P. Monnier, F. Raineri, B. B. Bakir, C. Seassal, R. Raj, and J. A. Levenson, *Phys. Rev. Lett.* **97**, 143904 (2006).
- [15] S. Barbay, R. Kuszelewicz, and A. M. Yacomotti, *Opt. Lett.* **36**, 4476 (2011).
- [16] M. Brunstein, A. M. Yacomotti, I. Sagnes, F. Raineri, L. Bigot, and A. Levenson, *Phys. Rev. A* **85**, 031803 (2012).
- [17] T. Van Vaerenbergh, M. Fiers, P. Mechet, T. Spuesens, R. Kumar, G. Morthier, B. Schrauwen, J. Dambre, and P. Bienstman, *Opt. Express* **20**, 20292 (2012).
- [18] S. Reitzenstein and A. Forchel, *J. Phys. D* **43**, 033001 (2010).
- [19] T. Elsass, K. Gauthron, G. Beaudoin, I. Sagnes, R. Kuszelewicz, and S. Barbay, *Eur. Phys. J. D* **59**, 91 (2010).
- [20] J. L. A. Dubbeldam, B. Krauskopf, and D. Lenstra, *Phys. Rev. E* **60**, 6580 (1999).
- [21] M. A. Larotonda, A. Hnilo, J. M. Mendez, and A. M. Yacomotti, *Phys. Rev. A* **65**, 033812 (2002).
- [22] M. Nahmias, B. Shastri, A. Tait, and P. Prucnal, *IEEE J. Sel. Top. Quantum Electron.* **19**, 1 (2013).
- [23] E. Izhikevich, *IEEE Trans. Neural Networks* **15**, 1063 (2004).
- [24] P. Couillet, D. Daboussy, and J. R. Tredicce, *Phys. Rev. E* **58**, 5347 (1998).
- [25] A. Dousse, J. Suffczyński, O. Krebs, A. Beveratos, A. Lemaître, I. Sagnes, J. Bloch, P. Voisin, and P. Senellart, *Appl. Phys. Lett.* **97**, 081104 (2010).
- [26] M. Abbarchi, A. Amo, V. G. Sala, D. D. Solnyshkov, H. Flayac, L. Ferrier, I. Sagnes, E. Galopin, A. Lemaître, G. Malpuech, and J. Bloch, *Nat. Phys.* **9**, 275 (2013).